

Detection of Cortical Oscillations Induced by SCS Using Power Spectral Density

Lukáš SVOBODA¹, Andrej STANČÁK², Pavel SOVKA¹

¹Dept. of Circuit Theory, Czech Technical University, Technická 2, 166 27 Prague 6, Czech Republic

²Dept. of Normal, Pathological and Clinical Physiology, Third Faculty of Medicine, Ke Karlovu 4, 120 00 Prague 2, Czech Republic

svobol4@fel.cvut.cz, sovka@fel.cvut.cz, stancak@lf3.cuni.cz

Abstract. *Chronic, intractable pain of lower back and lower extremity might develop as the result of unsuccessful surgery of back. This state called failed-back surgery syndrome (FBSS) cannot be effectively treated by pharmacotherapy. Electric stimulation of the dorsal spinal cord is applied to relieve the pain. According to the medical hypothesis, oscillatory activity, which might be related to the analgesic effects, may occur in the cortex during the stimulation. To confirm the presence of the SCS induced oscillations, a new method of detection was designed for this purpose. The analysis of EEG data was performed using power spectral density, confidence intervals, visualization and group statistic for its verification. Parameters of the method were experimentally optimized to maximize its reliability. During ongoing SCS, statistically significant changes were detected and localized at the stimulation frequency and/or its subharmonic or upper harmonic over central midline electrodes in eight patients.*

Keywords

Power spectral density, failed-back surgery syndrome, spinal cord stimulation, induced oscillations, EEG.

1. Introduction

Musculoskeletal disorders afflicted 13.2 % of Czech population aged 20–64 years in 2005 and represented 26.3 % of disability days. They became the most considerable cause of work disability even before respiratory disorders (24.1 % of disability days). The most numerous group of musculoskeletal disorders is composed of dorsopathies (69 %, diagnoses M43–M54 according to ICD-10), which, in most cases, are accompanied by pain [17].

Low back pain (M54.5) reduces the quality of life and disables about 50 % of afflicted people [2]. The cure is not always satisfactory, although the estimate of treatment costs was 24 billion dollars (USA, 1990), excluding workers compensation claims and lost of productivity.

Thus, chronic back pain became a great medical, but also social and economical problem.

Failed back surgery syndrome is the consequence of unsuccessful back surgery. It develops in about 15 % of cases [11], causing intractable chronic neuropathic pain in lower back and legs, which is, in most cases, resistant to pharmacotherapy [6]. Therefore, other methods were suggested to bring long-term pain relief. Since 1990s, an electric stimulation of the dorsal spinal cord (spinal cord stimulation – SCS) has been widely applied in FBSS treatment. Nowadays, the combination of SCS and chemical analgesics is the most effective way to alleviate the pain in FBSS.

The SCS therapy requires a stimulating electrode to be implanted into the spinal cord, usually in the area of 9th – 11th thoracic disk. The electrode is fixed with special clips and connected to an accumulator-powered generator using an extension lead. The electric excitation is performed by monophasic current pulses at 40–100 Hz over the period of several minutes followed by the rest period. In average, 59 % of patients reported that the intensity of pain perception was suppressed by 50 % or more in several studies [4]. The pain relief lasts for a few minutes even after the stimulation is terminated.

Analgesic effects of SCS are known for more than three decades and were documented in clinical studies [7], [9], but the mechanism of analgesia has not been reliably understood. It is supposed, that SCS spreads via spinal cord and thalamus to cortex, where it inhibits processing of pain in the pain matrix [1], [7], [9]. Cortical manifestations of spinal cord stimulation were already examined using fMRI in few patients [5], but the changes in electric activity of brain during SCS have not been researched yet.

In this paper, the design of the new method of detection of induced cortical oscillations is described. The interest is focused on the optimal selection of values of parameters needed for reliable computation of PSD, as well as on the verification of the results using group statistic. Also visualization is an important part of the method, due to the representation of the results intelligible to medical staff.

2. Pain and Analgesia

We discriminate between two types of pain regarding to its duration – acute pain and chronic pain. Acute pain generally signalizes an insult involving our body or its part. The purpose is to warn of the damage and elicit a reaction leading to removal of the painful cause. It usually lasts for days or weeks, rarely more than one month. On the other hand, chronic pain does not abate along with the primary cause, but persists at least for next 3–6 months. From the biological point of view, chronic pain is undesirable and produces only physical, psychical and social privation.

In case of acute pain, primary disease or injury has to be cured first and foremost as the cause of the pain. Moreover, there is also a need of alleviation of painful percepts at the same time. Otherwise, pathophysiological changes may occur, because the stress reaction of the body grows with the period of the pain and escalates a risk of change-over from acute to chronic phase. Fortunately, acute pain could be cured well, especially by chemical analgesics.

The methods of chronic pain treatment are different, because its causes are often not as clear as by acute pain. That's why a complete recovery may not be always possible. The main goal of the cure is a restoration of usual functions in physical, psychical and social sphere in attainable rate. Total effectiveness of chronic pain suppression could be increased using pharmacological and non-pharmacological therapy together [6]. One of non-pharmacological methods, that are successfully applied to alleviate some types of chronic pain, is spinal cord stimulation.

2.1 Stimulation of Dorsal Spinal Cord

Gating theory formulated in 1965 [8] stimulated a concern about the research of pain. The experiments led to the development of the first spinal cord stimulator, which was implanted to human already in 1967 [12]. However, little experience caused, that the method was applied without discrimination among different kinds of pain and the results did not fulfill expectations.

The SCS method returned to use at the end of eighties in last century. Nowadays, it asserts to alleviate the pain e.g. by peripheral vascular disease, reflex dystrophy of sympaticus, causalgiias, FBSS or angina pectoris [4]. Its

main advantage is the effectiveness in treatment of pain resistant to pharmacotherapy. The risks consist only in the limitations consequent on the usage of implanted device.

Stimulation electrode is introduced into the epidural space at dorsal side of spinal cord at the level of spinal roots innervating painful dermatoms. Using periodical current pulses (200–400 μ s long, repetition frequency 40 to 100 Hz) a paresthesia overlapping the painful area is induced. Stimulation current is supplied by the generator placed under the skin, usually in abdominal wall. Connection between electrode and generator is performed by implanted line wire. The patient can control the stimulation using external unit communicating wirelessly with the generator.

The experiences with suppression of pain in FBSS patients using SCS are very good. According to [15], 59 % patients indicated more than 50% long-term relief from pain. Other authors [10] observed a group of 153 patients with FBSS suffering from pain shooting to legs. Permanent stimulator was implanted by 87 % of them and 50 % showed notable pain relief.

3. Patients and EEG Data

Our study was based on the EEG recordings acquired from ten FBSS patients, suffering from intractable neuropathic pain located in their lower back and leg after unsuccessful back surgery. The pain was resistant to pharmacotherapy, hence an electric stimulation of dorsal spinal cord was applied to suppress it.

Tab. 1 shows gender and age of the patients in the study, localization and duration of neuropathic pain, placement of the tips of stimulation electrode, SCS frequency, SCS therapy duration and medication on the day of the measurement. The frequency of SCS ranged from 45 Hz to 100 Hz and, in each patient, it was set to the value ensuring maximal pain relief. The reduction of pain, compared to the pain experienced after several hours without stimulation, was reported at least 50 % in all patients.

The monopolar EEG was acquired continuously using 111 Ag/AgCl electrodes distributed equally on the scalp approximately 2.5 cm from one another with forehead as

Patient No.	Age [years]	Gender	Pain localization	Pain duration [months]	Stim. electrode location	Stim. frequency [Hz]	SCS duration [months]	Medication on the day of EEG recording
A01	50	M	left leg, back	132	Th11	60	35	tramadol
A02	39	M	left leg, back	48	Th10	45	18	tramadol
A03	39	F	left leg, back	96	Th10	100	43	tramadol
A04	41	M	right leg, back	38	Th10–11	60	20	tramadol
A05	51	M	left leg, back	84	Th9	100	40	DHC cont., ibuprofen
A06	37	F	left leg, back	108	Th10	85	12	none
A07	51	F	left leg, back	72	Th10	85	40	tramadol
A08	49	M	left leg, back	132	Th10	85	20	tramadol
A09	56	F	left leg, back	108	Th10	85	30	DHC cont., ibuprofen
A10	58	M	left leg, back	168	Th10	65	21	DHC cont., nimesulid

Tab. 1. Age and gender of patients participating the study, localization and duration of chronic pain, location of stimulation electrode, SCS frequency, SCS therapy duration and medication (M – male, F – female, Th – thoracic vertebra).

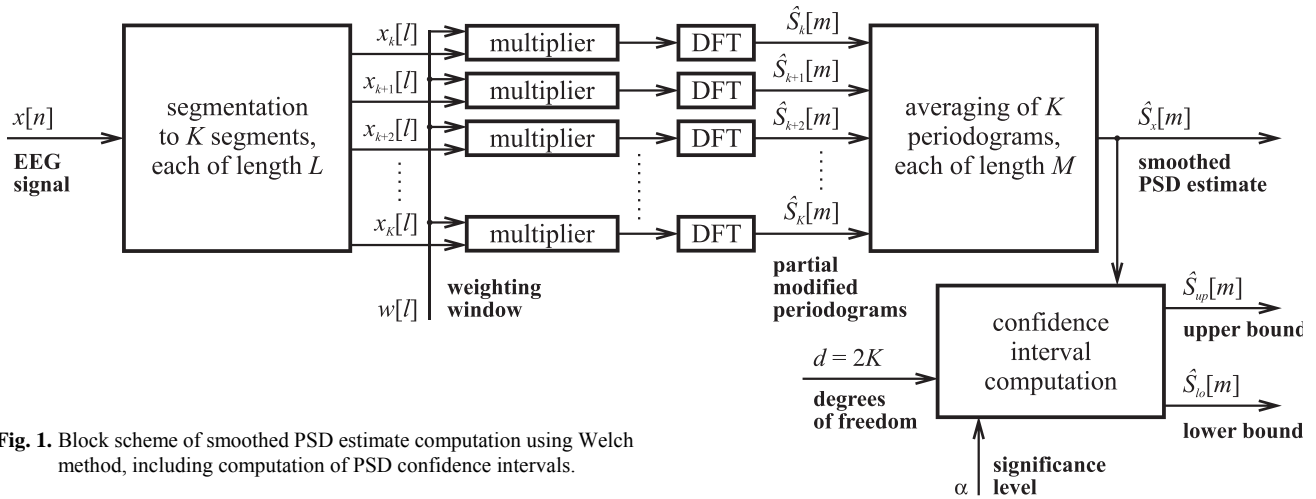


Fig. 1. Block scheme of smoothed PSD estimate computation using Welch method, including computation of PSD confidence intervals.

a reference. While recording EEG, the patients were sitting still in the comfortable armchair with their eyes closed. There were two EEG recordings from each patient – one recorded during ongoing SCS, second with no stimulation. The positions of electrodes were also measured. Vertical and horizontal electrooculogram were recorded bipolarly to identify artefacts in the recordings. All signals were filtered by anti-aliasing bandpass (0.015–200 Hz) and then digitized at 1024 Hz sampling frequency.

4. Method

The goal is to detect reliably, if there is a change of electrical activity in cortex, represented by EEG, during ongoing SCS. The method consists of four successive steps:

1. spectral analysis using Welch method for smoothed PSD estimate computation,
2. confidence intervals of PSD estimate to evaluate statistical significance of power change,
3. visualization of power difference (SCS on vs. SCS off) using pseudocolor scalp maps,
4. pair *t*-test to check general validity of power increase in the group of all patients.

4.1 Data Pre-processing

Digitized EEG recordings were visually checked for the presence of artefacts caused by eye and head motion or by muscle activity and affected segments were deleted. Monopolar data was spatially transformed using Laplace operator method [14] to amplify the influence of currents flowing radial to electrodes.

4.2 Spectral Analysis

We supposed that SCS generates an oscillatory activity in some parts of cortex, which were of the same frequency as the stimulation and could be found on the scalp.

A difference between PSDs of pair EEG recordings (measured in one patient with SCS on and SCS off respectively) denotes that stimulation has an influence over electrical activity of brain. If the power increase (compared to recording acquired with SCS off) occurs at stimulation frequency, it is probable that SCS induces cortical oscillations at the frequency equal to its own.

Smoothed estimate of power spectral density of stochastic signal represents the distribution of total probabilistic power among single “spectral lines”. Thus it may be used for comparison of power of two signals at distinct frequency. By each patient, the analysis was performed for signals coming from all 111 electrodes and all four EEG recordings (original monopolar data and spatially transformed data, both with SCS on and SCS off respectively). Thus the total number of processed time courses was 4440.

4.2.1 PSD Estimate

Power spectral density and computation of its estimate from measured data have been described in number of publications [3], [16]. Hence only the equations in discrete form are mentioned here, as they were used for analysis of our EEG recordings.

Consistent estimate of power spectral density was computed by Welch method. This direct technique, based on Fourier transform of weighted segments of input signal, is depicted in Fig. 1.

Input sequence $x[n]$ of length N is divided into K successive segments $x_k[l]$, each L samples long, thus $N=KL$. Every segment is then multiplied by specific type of smooth window $w[l]$ of identical length (we used Hamming window) and transformed into partial modified periodogram $\hat{S}_k[m]$ using DFT [3], [13]:

$$\hat{S}_k[m] = \frac{1}{W} \frac{T}{L} \left| \sum_{l=0}^{L-1} x[l+kL] \cdot w[l] \cdot e^{-j2\pi ml} \right|^2, \quad (1)$$

$$k \in \langle 0, K-1 \rangle, \quad K = \frac{N}{L},$$

where $x[l+kL]$ is the realization of $x_k[l]$ and

$$W = \frac{1}{L} \sum_{l=0}^{L-1} w^2[l]. \quad (2)$$

Thus we have K partial modified periodograms and after averaging them we get smoothed estimate:

$$\hat{S}_x[m] = \frac{1}{K} \sum_{k=0}^{K-1} \hat{S}_k[m]. \quad (3)$$

Averaging decreases total variance of the estimate K -times compared to periodogram computed from whole input sequence.

Power spectral density computed using equation (3) was transformed into decibel scale:

$$\hat{S}_{x\text{dB}}[m] = 10 \log \hat{S}_x[m] \quad [\text{dB}]. \quad (4)$$

4.2.2 Confidence Intervals

In accordance to generally used assumption, a sequence of EEG signal samples is normally distributed. Hence its Fourier transform (real and imaginary part) is normally distributed, because it is a linear transform.

If we divide an input sequence $x[n]$ into K segments, during averaging we sum up K random variables with χ^2_d distribution. That's why the smoothed estimate is of χ^2_d distribution with $d=2K$ degrees of freedom.

Confidence interval for smoothed estimate of power spectral density can be defined [3], [13]:

$$\Pr \left\{ \frac{d\hat{S}_x[m]}{\chi^2_{d; 1-\frac{\alpha}{2}}} \leq S_x[m] \leq \frac{d\hat{S}_x[m]}{\chi^2_{d; \frac{\alpha}{2}}} \right\} = 1 - \alpha, \quad (5)$$

where $\Pr\{ \}$ denotes the probability of the event in curly brackets, $d=2K$ is the number of degrees of freedom and α represents the significance level determining the probability of the state that the real value $\hat{S}_k[m]$ occurs outside the computed interval (we used $\alpha = 0.05$). The symbols $\chi^2_{d; \frac{\alpha}{2}}$ and $\chi^2_{d; 1-\frac{\alpha}{2}}$ denote critical values of χ^2 distribution with d degrees of freedom at significance level $\frac{\alpha}{2}$.

The equation (5) describes confidence interval of one "spectral line". If the power spectrum is in decibel (logarithmic) scale according to equation (4), the interval is equal for all frequencies [3], [13]:

$$\Pr \left\{ \hat{S}_{x\text{dB}}[m] + 10 \log \frac{d}{\chi^2_{d; 1-\frac{\alpha}{2}}} \leq S_{x\text{dB}}[m] \leq \hat{S}_{x\text{dB}}[m] + 10 \log \frac{d}{\chi^2_{d; \frac{\alpha}{2}}} \right\} = 1 - \alpha. \quad (6)$$

With increasing degree of freedom d , χ^2 distribution converges to normal distribution with mean d and variance $2d$ [3]. If the signal is long enough and could be divided

into sufficient number of segments ($K \geq 30$, thus $d \geq 60$), the distribution of the smoothed power spectrum could be properly approximated by normal distribution at the same significance level. The equations, which can be used for approximation of confidence intervals of PSD estimate, could be found in Appendix of this article.

4.3 Parameters of Computation

The properties of PSD estimate are influenced with the selection of parameters, such as weighting window, segment length, overlap between adjacent segments or number of discrete frequencies, for which power spectrum is computed.

The values of parameters should result from three general contradictory requests on PSD estimate:

- high frequency resolution of PSD,
- low leakage of energy,
- narrow confidence interval.

There are several variables featuring in the computation. The first three are given by the measurement and physiology:

- $x[n]$ is the EEG signal coming from one electrode.
- $x_k[l]$ is the segment of $x[n]$ and its length L is determined by the request of the doctors resulting from physiology.
- f_s represents sampling frequency of $x[n]$ in hertz, which is given by the measuring device used in the experiment. It has no direct influence on PSD computation, but is important for the selection of other parameters.

Remaining parameters have to be chosen:

- $w[l]$ is the weighting window; each segment $x_k[l]$ is multiplied by $w[l]$ to reduce leakage of energy. The leakage would decrease "contrast" between single "spectral lines" and weighting reduces this undesirable event. The length of the window L is the same as the length of $x_k[l]$.
- n_{FFT} means number of discrete frequencies, in which PSD estimate is computed. It is suitable to choose n_{FFT} as power of two, preferably identically as the length of $x_k[l]$, because of no need of interpolation in spectra. For EEG (real input signal), the length of resulting power spectrum is $\frac{n_{FFT}}{2} + 1$.
- \circ is an overlap between adjacent segments. It ranges from zero to $L-1$. Total number of samples of each EEG recording is finite. If a narrow confidence interval is needed, also the number of segments has to be high. The more periodograms we average, the lower is the variance of the smoothed estimate. Using overlap, the number of partial modified periodograms

Input	Parameters					Outputs (size)	
	f_s	$w[l]$ (type, size)	n_{FFT}	o	p	$\hat{S}_x[m]$	$c_i[m]$
SCS on	1024	Hamming, 1024	1024	0	–	1×513	–
SCS off	1024	Hamming, 1024	1024	0	0.95	1×513	2×513

Tab. 2. Input parameters and outputs of PSD estimate and confidence intervals computation.

that enter averaging, can be increased, if needed. Overlapping can partially eliminate the effect of weighting window, but also increases dependence of the segments.

- p represents the probability, with which real PSD values $S_x[m]$ lay in computed confidence interval $c_i[m]$. It holds $p=1-\alpha$, where α is a level of significance.

4.3.1 Selection of Parameters

The final values of parameters used for the computation of the power spectra of the EEG and the sizes of output matrices are listed in Tab. 2. They were selected so, that the requests on PSD estimate stated in 4.3 are taken into account.

The value of sampling frequency of EEG recordings $f_s=1024$ Hz is given by measuring device, which determines the range of frequencies in the digitized signal (0–512 Hz, according to Shannon theorem).

Thus, the segment $x_k[l]$ of one second duration (request of the doctors) includes $L = 1024$ samples. Average length of artefact-free recordings is $N=117.6\pm 36$ seconds (mean \pm SD), so the number of segments is more than sufficient ($N\geq 30$) and there is no need of overlap.

Frequency resolution depends primarily on the ratio f_s/n_{FFT} . Hence, the value of n_{FFT} should be high. On the other hand, weighting window and single segments should be of the length n_{FFT} . Thus, the value $n_{FFT} = 1024$ resulting in 1 Hz frequency resolution is determined by the length of the segment L .

To reduce leakage of the energy, shape of the weighting window has to be non-rectangular. There is an acceptable compromise between the improvement of adjacent lines “contrast” and the frequency resolution decrease, if we use Hamming window. The attenuation of the lobe adjacent to the main one is 42.7 dB and the frequency resolution drops to one half.

The probability p is given by such type of medical studies: $p = 0.95$. The confidence intervals were computed

only for the recordings acquired with SCS off. The variable $c_i[m]$ consists of two vectors – lower bound and upper bound of 95% two-tailed confidence interval for each of 513 “spectral lines”.

5. Results

In each patient, the power spectra from all electrodes were visually checked to identify significant power increase at stimulation frequency during the SCS.

In eight of ten patients, statistically significant power increase was found at the stimulation frequency and/or its harmonic or subharmonic. For every patient, Tab. 3 shows the value of stimulation frequency, declared by doctors, the frequency ascertained from computed power spectra and the number of electrode, where maximal difference between PSD with SCS on and PSD with SCS off was found.

5.1 Frequency Courses of PSD

In Fig. 2, there are power spectral densities of spatially filtered EEG signals coming from electrodes listed in the last row of Tab. 3 for frequency range 10–150 Hz and first five patients. Power spectral density of EEG with stimulation off is depicted in blue, its confidence interval in green and power spectrum with SCS on in red. Declared stimulation frequency is marked by black dotted line. The frequency, at which maximal power increase (during SCS) occurred, is marked by the red arrow.

The highest increase (during SCS on) appeared in power spectra of patients A01, A02, A07 and A08. On the contrary, no significant difference was found in PSD of the EEG recorded in patients A05 and A09. Either spinal cord stimulation did not induce oscillations in cortex, or the oscillations were not so intensive to be considered as statistically significant.

Furthermore, the analysis of power spectra of patients A03 and A05 was a bit problematic, because declared stimulation frequency 100 Hz may interfere with second harmonic of supply network.

Patient number	A01	A02	A03	A04	A05	A06	A07	A08	A09	A10
Stim. frequency declared [Hz]	60	45	100	60	100	85	85	85	85	65
Stim. frequency measured [Hz]	62	45	89	29	–	83	84	84	–	64
Electrode number	50	50	37	50	38	51	50	37	50	77

Tab. 3. Declared and measured values of stimulation frequency and electrodes with highest power difference at this frequency.

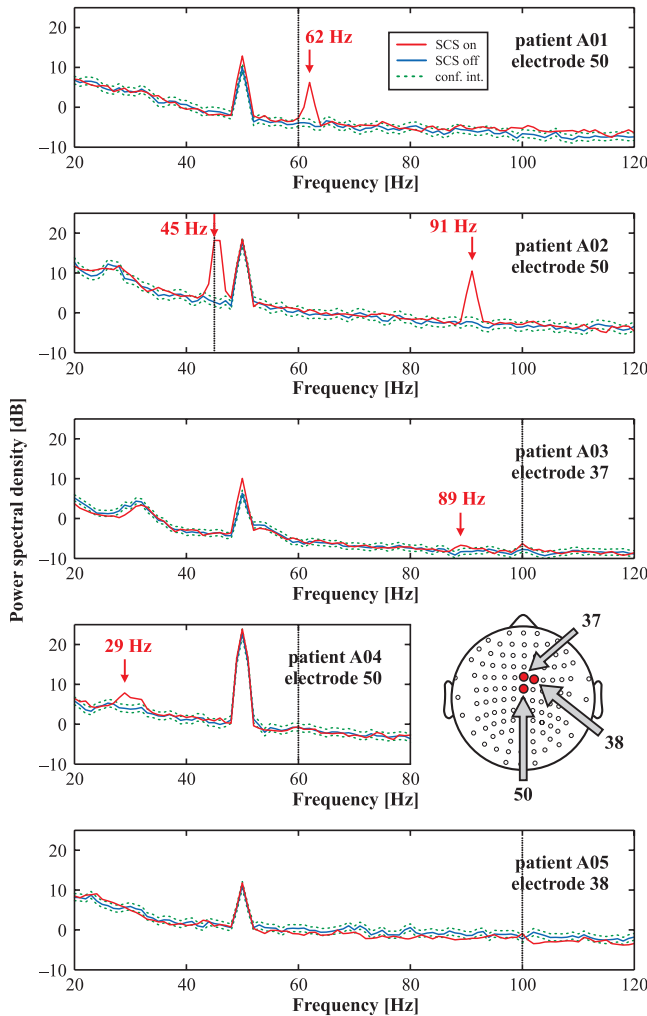


Fig. 2. Power spectra with the highest power difference at measured stimulation frequency (patients 1–5).

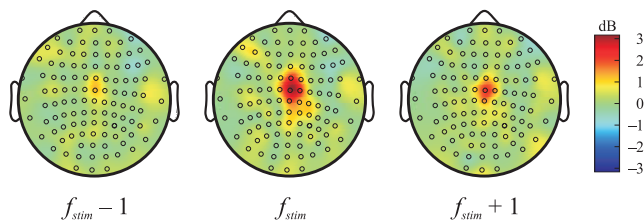


Fig. 3. Scalp projections of difference of power spectra at measured stimulation and two adjacent frequencies (all patients grand average).

In patients A03, A06 and A10, power spectrum with SCS on exceeded confidence interval of PSD with SCS off at the frequencies not exactly identical as declared ones, but very close to these values (2–3 Hz maximal difference). The power difference, although it was statistically significant, achieved only little values in this case. Hence it could not be certainly asserted, that cortical oscillations are a consequence of SCS. It might be caused e.g. by general mutual shift of spectra or by noise. The reason may also be the higher variance of PSD values with SCS on, which accordingly exceed borders of significance interval computed from PSD with SCS off (whose variance is lower).

5.2 Surface Maps of PSD

Scalp projection of the power difference between PSD with SCS on and PSD with SCS off respectively is depicted in Fig. 3. The surface maps were computed as averages of differential power spectral density maps of all ten patients at measured stimulation frequency f_{stim} and closely adjacent frequencies $f_{stim}-1, f_{stim}+1$ [Hz]. These maps show the fact, that cortical oscillations, occurring as the consequence of SCS, are localized identically in all patients, namely in the central part of the scalp, under the electrodes 37, 50, 51 and 63. Statistically nonsignificant differential values included in confidence interval were set to zero.

5.3 Group Statistic

The hypothesis that spinal cord stimulation induces oscillations in central medial part of cortex at stimulation frequency was tested using pair t -test.

In each patient, the electrode with the highest power difference between PSD with SCS on and PSD with SCS off was picked up. The dataset consists of ten pairs (S_s^*, S_n^*) , where S_s^* is a value of PSD with SCS on and S_n^* is a value of PSD with SCS off. Input data are listed in the Tab. 4.

Normal distribution of random samples S_s^* and S_n^* was checked using Lilliefors' test of normality at 1% significance level.

Statistical significance of the difference $S_s^* - S_n^*$ in the group of all patients was proven at significance level $\alpha = 0.05$. The number of degrees of freedom ensued from dataset was 9 (number of patients minus one). The value of test statistic was $T = 2.78$, while critical value of Student distribution fractile was $t_c = 1.83$, hence the power increase during SCS is statistically significant in the whole group of patients.

Patient No.	Declared f [Hz]	Detected f [Hz]	Electrode No.	Power spectral density [dB]		
				S_s^*	S_n^*	$S_s^* - S_n^*$
P01	60	62	50	6,214	-4,002	10,216
P02	45	45	50	18,170	2,739	15,431
P03	100	89	37	-6,691	-8,312	1,621
P04	60	29	50	7,867	4,007	3,860
P05	100	-	38	-0,932	-2,290	1,358
P06	85	83	51	0,749	-1,280	2,029
P07	85	84	50	-1,291	-4,073	2,782
P08	85	84	37	2,540	-2,945	5,485
P09	85	-	50	-3,036	-2,665	-0,371
P10	65	64	77	1,051	0,191	0,860

Tab. 4. Maximal power differences at detected stimulation frequency.

6. Conclusion

The detection of induced cortical oscillations in EEG using the method described in this paper has not been previously performed. This study is also the first to show effects of SCS on the electric oscillatory activity of the human brain.

The results showed that induced oscillations in primary somatosensory cortex representing foot come up as the effect of electrical stimulation of dorsal spinal cord. Statistically significant power increase at stimulation frequency (or its harmonic or subharmonic frequency) on electrodes in central part of the scalp was found during SCS in eight of ten FBSS patients.

No statistically significant power increase occurred in two patients (at 85 and 100 Hz), although the pain relief was reported by these patients during SCS and after it. There are more possible reasons, but two main causes may be assumed – interference with power supply (its second harmonic component) at 100 Hz and stronger damping of SCS-induced oscillations due to their higher frequency that transmits less energy than low-frequency oscillations.

Our method may be used for detection of presence of induced electrical activity in EEG signal. Smoothed power spectral density combined with confidence intervals and pseudocolor scalp visualization is a reliable tool, which can easily reveal significant power change in spectrum. A pair t -test then proves general validity of the findings that may contribute to explanation of the mechanism of SCS action and could in future be used to optimize stimulation parameters, e.g. frequency, current strength and optimal position for implantation of the stimulation electrode.

7. Appendix

7.1 Two-Tailed Confidence Interval

Two-tailed confidence interval is a zone lining the estimate of random quantity, in which a real value of the quantity lays (with some high probability – e.g. 95–99 %).

If a random signal $\{x_k[n]\}$ is normally distributed, then its Fourier transform (both real and imaginary part) is normally distributed too, because it is a linear transform. Discrete periodogram computed using one complete realization of the signal $x[n]$ is described by the equation

$$\hat{S}_x[e^{j\Omega}] = \frac{T}{N} \left| \sum_{n=0}^{N-1} x[n] \cdot e^{-j\Omega n} \right|^2 \quad (7)$$

where $\Omega = 2\pi/T$ is a discrete frequency, $T=1/f_s$ a period and N a number of samples of $x[n]$. Hence each “spectral line” is of χ^2 distribution with two degrees of freedom ($d=2$). Single “spectral lines” represent an estimate of the signal variance $\hat{\sigma}_x^2$ at related frequency. It holds:

$$\frac{2\hat{\sigma}_x^2}{\sigma_x^2} = \frac{2\hat{S}_x[m]}{S_x[m]} = \chi_2^2 \quad (8)$$

where $\hat{\sigma}_x^2$ is an estimate of the variance σ_x^2 of the random signal $x[n]$. From (8), it follows that the distribution of the random error of the estimate is independent on the length of the realization, from which the estimate was computed.

If the input sequence $x[n]$ is divided into K segments, K random variables with χ_2^2 distribution are summed up while averaging. Thus, the smoothed estimate $\hat{S}_x[m]$ computed using (3) is of χ_d^2 distribution with $d=2K$ degrees of freedom and its random error is \sqrt{K} -times lower compared to the periodogram according to (7).

7.2 Approximation of Confidence Intervals of PSD Estimate Using $N(0, 1)$ Distribution

If the number of degrees of freedom d is high enough ($d>60$), χ^2 distribution could be approximated by normal distribution $N(d, 2d)$, so it holds:

$$\begin{aligned} \chi_{d; 1-\frac{\alpha}{2}}^2 &\doteq q_{1-\frac{\alpha}{2}} \\ \chi_{d; \frac{\alpha}{2}}^2 &\doteq q_{\frac{\alpha}{2}} = -q_{1-\frac{\alpha}{2}} \end{aligned} \quad (9)$$

where $q_{1-\frac{\alpha}{2}}$ and $q_{\frac{\alpha}{2}}$ are quartiles of normal distribution $N(d, 2d)$. However, they are not tabulated, hence we transform them using standard normal distribution $N(0,1)$. The equations (9) then switch into the terms:

$$\begin{aligned} \chi_{d; 1-\frac{\alpha}{2}}^2 &\doteq d + u_{1-\frac{\alpha}{2}} \sqrt{2d} \\ \chi_{d; \frac{\alpha}{2}}^2 &\doteq d - u_{1-\frac{\alpha}{2}} \sqrt{2d} \end{aligned} \quad (10)$$

where $u_{1-\frac{\alpha}{2}}$ is a quartile of standard normal distribution $N(0,1)$ and $d=2K$ is a number of degrees of freedom equal to the doubled number of segments.

After introducing the equations (10) into the term (5):

$$\begin{aligned} \Pr \left\{ \frac{d\hat{S}_x[m]}{d + u_{1-\frac{\alpha}{2}} \sqrt{2d}} \leq S_x[m] \leq \right. \\ \left. \leq \frac{d\hat{S}_x[m]}{d - u_{1-\frac{\alpha}{2}} \sqrt{2d}} \right\} = 1 - \alpha \end{aligned} \quad (11)$$

and after rearrangement:

$$\begin{aligned} \Pr \left\{ \frac{\hat{S}_x[m]}{1 + u_{1-\frac{\alpha}{2}} \sqrt{\frac{2}{d}}} \leq S_x[m] \leq \right. \\ \left. \leq \frac{\hat{S}_x[m]}{1 - u_{1-\frac{\alpha}{2}} \sqrt{\frac{2}{d}}} \right\} = 1 - \alpha \end{aligned} \quad (12)$$

Acknowledgements

The research was supported by the project of the Czech Ministry of Education MSM 6840770012 “Transdisciplinary Research in Biomedical Engineering 2”, MSM 0021620816 and IGA NF 8232/3. We are grateful to Dr. Kozák and Dr. Vrba for providing patient volunteers and to Dr. Vrána and Dr. Poláček for their help during data recording.

References

- [1] ALÓ, K. M., HOLSHEIMER, J. New Trends in Neuromodulation for the Management of Neuropathic Pain. *Neurosurgery*. April 2002, vol. 50, no. 4, pp. 690–704.
- [2] BELL, G. K. KIDD, D., NORTH, R. B. Cost-Effectiveness Analysis of Spinal Cord Stimulation in Treatment of Failed Back Surgery Syndrome. *Journal of Pain and Symptom Management*. May 1997, vol. 13, no. 5, pp. 286–295.
- [3] BENDAT, J. S., PIERSOL, A. G. *Random Data: Analysis and Measurement Procedures*. New York: John Wiley & Sons, 1971. ISBN 0-471-06470-X.
- [4] KEMLER, M. A. Spinal Cord Stimulation and Pain. *Epilepsy & Behavior*. 2001, vol. 2, no. 3, pp. 88–94.
- [5] KIRIAKOPOULOS, E.T. et al. Functional Magnetic Resonance Imaging: A Potential Tool for the Evaluation of Spinal Cord Stimulation: Technical Case Report. *Neurosurgery*. August 1997, vol. 41, no. 2, pp. 501–504.
- [6] KOZÁK, J. et al. Methodical Instructions for Acute and Chronic Non-Oncogenous Pain Pharmacotherapy (in Czech). *Bolest*. 2004, vol. 7, sup. 1, pp. 9–18.
- [7] LINDEROTH, B., MEYERSON, B. A. Central Nervous System Stimulation for Neuropathic Pain. In *Neuropathic Pain: Pathophysiology and Treatment*. Seattle: IASP Press, 2001, pp. 223–249. ISBN 0-931092-38-8.
- [8] MELZACK, R., WALL, P. D. Pain Mechanisms: A New Theory. *Science*. November 1965, vol. 150, no. 699, pp. 971–979.
- [9] MEYERSON, B. A., LINDEROTH, B. Spinal Cord Stimulation: Mechanisms of Action in Neuropathic and Ischaemic Pain. In *Electrical Stimulation and the Relief of Pain*. Amsterdam: Elsevier Science, 2003, pp. 161–182.
- [10] NORTH, R. B. et al. Spinal Cord Stimulation for Chronic, Intractable Pain: Experience Over Two Decades. *Neurosurgery*. March 1993, vol. 32, no. 3, pp. 384–394.
- [11] PALEČEK, P., MRŮZEK, M. Failed Back Surgery Syndrome (in Czech). *Neurologie pro praxi*. 2003, vol. 3, no. 6, pp. 315–318.
- [12] SHEALY, C. N., MORTIMER, J. T., RESWICK, J. B. Electrical Inhibition of Pain by Stimulation of the Dorsal Columns: Preliminary Report. *Anesthesia and Analgesia*. July 1967, vol. 46, no. 4, pp. 489–491.
- [13] SVOBODA, L. *Detection of Electrocortical Rhythms Induced by Spinal Neurostimulator in Patients Suffering from Chronic Pain* (in Czech). Diploma thesis. Prague: FEE CTU, Dept. of Circuit Theory, 2006.
- [14] THICKBROOM, G. W. et al. Source Derivation: Application to Topographic Mapping of Visual Evoked Potentials. *Electroencephalography and Clinical Neurophysiology*. July 1984, vol. 4, no. 59, pp. 279–285.
- [15] TURNER, J. A., LOESER, J. D., BELL, K. G. Spinal Cord Stimulation for Chronic Low Back Pain: A Systematic Literature Synthesis. *Neurosurgery*. December 1995, vol. 37, no. 6, pp. 1088–1095.
- [16] WELCH, P. D. The Use of Fast Fourier Transform for the Estimation of Power Spectra: A Method Based on Time Averaging over Short, Modified Periodograms. *IEEE Transactions on Audio & Electroacoustics*. June 1967, vol. 15, no. 2, pp. 70–73.
- [17] *Terminated Cases of Incapacity for Work for Disease or Injury 2005*. Prague: ÚZIS, 2006. ISBN 80-7280-535-5.

About Author...

Lukáš SVOBODA was born in 1982 in Prague. He graduated at CTU FEE in 2006, Biomedical Engineering program, and continues as a post-gradual student at the Department of Circuit Theory, CTU FEE, where he works on EEG signal processing and analysis.

Call for Papers

Advanced Electronic Circuits

• from analog to digital • from low frequencies to millimeter waves •

A Special Issue of

Radioengineering

Submission of a paper: October 15, 2008